Stability of planar reactive fronts in external fields

Arkady B. Rovinsky,* Anatol M. Zhabotinsky,† and Irving R. Epstein‡
Department of Chemistry and Volen Center for Complex Systems, Brandeis University, Waltham, Massachusetts 0254-9110
(Received 17 June 1998)

Differential flows of species, which may arise in reactive systems due to external fields such as electric fields or pressure gradients, may significantly affect the characteristics and stability of propagating fronts. A generalized Kuramoto-Sivashinsky equation describing the dynamics of perturbations of a planar front in systems with differential flows is derived and analyzed. The analysis shows that a differential flow parallel to the front may have either a destabilizing or a stabilizing effect. The effect of a lateral flow does not depend on its direction, while normal flows have a stabilizing effect when running in one direction and a destabilizing effect in the other. These analytical conclusions are verified in numerical experiments with a model of a cubic autocatalytic reaction. As a result of the instability, a periodic pattern of modulation appears on the front. In the case of lateral flow, the pattern drifts along the front. With normal flow, the pattern is stationary. The simulations show that both lateral and normal differential flows have a significant effect on the front velocity. [S1063-651X(98)08611-5]

PACS number(s): 03.40.Kf, 82.20.Mj, 42.25.Gy

I. INTRODUCTION

In a variety of spatially extended systems, such as flames, solidification fronts, waves of excitation in biological media, and chemical waves [1–3], one may observe moving fronts that separate parts of the medium in different states. The stability of such fronts is an important problem. A key factor that affects a front's stability is transport. Transport provides the coupling between spatially separated elements and brings about the front propagation. Of the two kinds of transport, convective and diffusive, diffusive transport has been far more extensively considered in studies of front stability.

Homogeneous flows can arise naturally in systems subjected to external fields, such as electric fields or pressure gradients. As such fields may unequally affect the components of the system (e.g., ions of opposite charge), the flow velocities of the various components may be different. The ''differential flow'' of the constituents may change the stability of the system's homogeneous steady state and lead to the appearance of patterns [4].

Here, we study the effect of external fields and the resulting differential flows on the stability of propagating planar fronts. It is known that electric fields may profoundly influence traveling waves in biological tissues [5], chemical reactions [6], and combustion processes [7]. It appears, however, that no general approach has been developed to describe the observed phenomena. This work outlines such an approach by generalizing the Kuramoto-Sivashinsky description [8] of wave fronts.

Since differential flows can only be produced by, and are proportional to, external fields, we use the terms ''differential flow'' and ''external field'' interchangeably (assuming here that a field gives rise only to differential flows). The effects of an external field differ significantly for the lateral (i.e., parallel to the front) and normal components of the field. The effect of the lateral component is quadratic in the field strength and may be either destabilizing or stabilizing, depending on the details of the system and the wave regime under consideration. The effect of the normal component is linear. As a result, normal fields of opposite directions always have opposite effects on the stability of the front. While these findings might be anticipated on the basis of symmetry considerations, they are deduced below from the explicit expression for the analog of the Kuramoto-Sivashinsky equation for systems in external fields. Our results are then verified by numerical experiments on a chemical model of cubic autocatalysis [10]. The numerical modeling also shows a strong effect of the differential flow on the front velocity.

Section II presents the theoretical description of differential flow effects. Section III describes the model and gives the results of numerical simulations. Numerical procedures are described in Sec. IV. Section V is devoted to discussion.

II. THE KURAMOTO-SIVASHINSKY EQUATION FOR SYSTEMS WITH DIFFERENTIAL FLOWS

We derive here the Kuramoto-Sivashinsky equation for systems in a constant uniform external field, using an adaptation of the original Kuramoto approach [9] suggested by Malevanets *et al.* [11]. The resulting equation governs the evolution of small, smooth perturbations of a planar front.

We assume that the external field causes advection of the components of the system. In an electric field, the flow velocity of each species is proportional to its electric charge, its mobility, and the field strength (Ohm's law). For a liquid phase in a porous medium, the flow velocity of a species is proportional to the pressure gradient (Darcy's law) and inversely proportional to the species' affinity to the solid phase. The reaction-diffusion-convection system is described by the equation

$$\dot{\mathbf{Z}} = \mathbf{f}(\mathbf{Z}) - (\vec{\mathbf{V}}\nabla)\mathbf{Z} + \mathbf{D}\Delta\mathbf{Z}, \tag{1}$$

*Electronic address: rovinsky@brandeis.edu
†Electronic address: zhabotinsky@brandeis.edu
‡Electronic address: epstein2@brandeis.edu

 © 1998 The American Physical Society

where $\mathbf{Z}$ is an n vector of phase variables, $\mathbf{f}(\mathbf{Z})$ is the kinetic term determined by the local interactions (in chemical systems given by the rate equations), $\mathbf{D}$ is a diagonal diffusivity matrix, and $\vec{\mathbf{V}}$ is a diagonal flow velocity matrix. $\vec{\mathbf{V}}$ is a matrix in the phase space whose elements are three-dimensional (3D) vectors in the physical space; it can be represented as $\mathbf{U}\vec{E}$, where $\mathbf{U}$ is an $n\times n$ diagonal mobility matrix and $\vec{E}$ is the 3D vector of the external field.

We assume that in one dimension Eq. (1) has a stable propagating front solution $\mathbf{Z}(t,x)=\mathbf{Z}_0(x-ct)$, where c is the front velocity. In other words, $\mathbf{Z}_0(\xi)$ is assumed to be a solution of the equation

$$-c\mathbf{Z}_0'=\mathbf{f}(\mathbf{Z}_0)-\mathbf{V}_x\mathbf{Z}_0'+\mathbf{D}\mathbf{Z}_0'', \tag{2}$$

where $\xi\equiv x-ct$ and the prime represents differentiation with respect to $\mathbf{Z}_0$'s single argument. We will be considering an infinite parametrically homogeneous medium. This implies translation invariance of the system: if $\mathbf{Z}_0(\xi)$ is a solution of Eq. (2) then, for any $d\xi$, $\mathbf{Z}_0(\xi+d\xi)$ is a solution as well. This implies that

$$\frac{\partial\mathbf{f}}{\partial\mathbf{Z}}(\mathbf{Z}_0)\mathbf{Z}_0'+(c-\mathbf{V}_x)\mathbf{Z}_0''+\mathbf{D}\mathbf{Z}_0'''=\mathbf{0}. \tag{3}$$

Let us designate $\mathbf{w}_0=\mathbf{Z}_0'(\xi)$. We will be using the solutions of the eigenvalue problem

$$\frac{\partial\mathbf{f}}{\partial\mathbf{Z}}(\mathbf{Z}_0)\mathbf{w}_i+(c-\mathbf{V}_x)\mathbf{w}_i'+\mathbf{D}\mathbf{w}_i''=\lambda_i\mathbf{w}_i, \tag{4}$$

and $\mathbf{w}_0$ is thus the eigenfunction of the problem corresponding to $\lambda_0=0$. Since for small shifts $d\xi$, $\mathbf{Z}_0(\xi+d\xi)=\mathbf{Z}_0(\xi)+(d\mathbf{Z}_0/d\xi)d\xi\equiv\mathbf{Z}_0(\xi)+\mathbf{w}_0d\xi$, a superposition of $\mathbf{Z}_0$ with a small perturbation along the $\mathbf{w}_0$ vector can be considered as a shifted solution $\mathbf{Z}_0(\xi+d\xi)$.

The last remark implies that a perturbed front solution can be sought in the form

$$\mathbf{Z}(x,y,z,t)=\mathbf{Z}_0[\xi+\psi_0(y,z,t)]+\sum_{i>0}\psi_i(y,z,t)\mathbf{w}_i(\xi). \tag{5}$$

Substituting expression (5) into Eq. (1) and using Eq. (2) yields

$$\sum_{i=0}^{\infty}\frac{\partial\psi_i}{\partial t}\mathbf{w}_i=\sum_{i=0}^{\infty}\left(\frac{\partial\mathbf{f}}{\partial\mathbf{Z}}(\mathbf{Z}_0)\mathbf{w}_i+(c-\mathbf{V}_x)\mathbf{w}_i'+\mathbf{D}\mathbf{w}_i''\right)\psi_i+\sum_{i=0}^{\infty}\mathbf{D}\mathbf{w}_i\Delta\psi_i+\mathbf{D}\mathbf{w}_0'(\nabla\psi_0)^2-\sum_{i=0}^{\infty}\vec{\mathbf{V}}\mathbf{w}_i\nabla\psi_i, \tag{6}$$

where

$$\mathbf{Z}_0=\mathbf{Z}_0(\xi+\psi_0),\quad \mathbf{w}_0=\mathbf{w}_0(\xi+\psi_0),\quad \text{and}\quad \mathbf{w}_i=\mathbf{w}_i(\xi),\quad i>0. \tag{7}$$

It should be noted that up to the terms of order $(\nabla\psi_0)^2$ Eq. (4) is satisfied and $\langle\mathbf{w}_0|\mathbf{w}_i\rangle=0$ with $\mathbf{Z}_0$ and $\mathbf{w}_i$ $(i=0,1,\dots)$ given by Eq. (7) [9,11]. With Eq. (4), Eq. (6) reduces to

$$\sum_{i=0}^{\infty}\frac{\partial\psi_i}{\partial t}\mathbf{w}_i=\sum_{i=0}^{\infty}\lambda_i\mathbf{w}_i\psi_i+\sum_{i=0}^{\infty}\mathbf{D}\mathbf{w}_i\Delta\psi_i+\mathbf{D}\mathbf{w}_0'(\nabla\psi_0)^2-\sum_{i=0}^{\infty}\vec{\mathbf{V}}\mathbf{w}_i\nabla\psi_i. \tag{8}$$

Since the functions ψ_i depend only on the y and z spatial coordinates, the operators ∇ and Δ can be thought of as acting only on those coordinates. For this reason only the $\mathbf{V}_y$ and $\mathbf{V}_z$ components of the flow (or external field) appear in Eq. (8). Therefore until otherwise specified we will think of $\vec{\mathbf{V}}$ as a lateral flow (i.e., in the frontal plane).

Taking scalar products of Eq. (8) with each of the left eigenvectors $\mathbf{w}_0^+(\xi+\psi_0)$ and $\mathbf{w}_i^+(\xi)$ $(i>0)$ yields the system of equations:

$$\frac{\partial\psi_i}{\partial t}=\lambda_i\psi_i+\sum_{j=0}^{\infty}D_{ij}\Delta\psi_j+d_{i0}(\nabla\psi_0)^2-\sum_{j=0}^{\infty}\vec{V}_{ij}\nabla\psi_j, \tag{9}$$

where $D_{ij}=\langle\mathbf{w}_i|\mathbf{D}|\mathbf{w}_j\rangle$, $d_{i0}=\langle\mathbf{w}_i|\mathbf{D}|\mathbf{w}_0'\rangle$, $\vec{V}_{ij}=\langle\mathbf{w}_i|\vec{\mathbf{V}}|\mathbf{w}_j\rangle$, and $\mathbf{w}_0=\mathbf{w}_0(\xi)$. Consider now the evolution of a small spatially smooth perturbation such that all ψ_i are initially of the same order of magnitude $\sim\psi$. By a spatially smooth perturbation we mean that any spatial derivative $|\nabla\psi|\ll|\lambda\psi|$, $|\lambda|=\min(|\lambda_1|,|\lambda_2|,\dots)$. Hence, the modes ψ_i $(i>0)$ evolve much faster than ψ_0 (which corresponds to $\lambda_0=0$), and therefore they can be adiabatically eliminated. In other words, these modes can be taken as solutions of the equations

$$\lambda_i\psi_i+\sum_{j>0}D_{ij}\Delta\psi_j-\sum_{j>0}\vec{V}_{ij}\nabla\psi_j=-D_{i0}\Delta\psi_0-d_{i0}(\nabla\psi_0)^2+\vec{V}_{i0}\nabla\psi_0,\quad i>0. \tag{10}$$

As the gradient terms on the left hand side of Eq. (10) are small compared to $\lambda_i\psi_i$, they can be neglected to a first approximation. In the second approximation the solution is

$$\psi_i=\frac{1}{\lambda_i}\left[\vec{V}_{i0}\nabla\psi_0-\left(D_{i0}-\sum_{j>0}\frac{\vec{V}_{ij}\vec{V}_{j0}}{\lambda_j}\right)\Delta\psi_0-\left(\sum_{j>0}\frac{D_{ij}\vec{V}_{j0}+\vec{V}_{ij}D_{j0}}{\lambda_j}-\sum_{j>0,k>0}\frac{\vec{V}_{ij}(\vec{V}_{jk}\vec{V}_{k0})}{\lambda_j\lambda_k}\right)\nabla^3\psi_0\right],\quad i>0. \tag{11}$$

Substituting ψ_i into Eq. (9) for ψ_0 and making the transformation of coordinates $y\mapsto y-V_{00,y}t$, $z\mapsto z-V_{00,z}t$, we finally arrive at the Kuramoto-Sivashinsky equation for systems in external fields:

$$\frac{\partial\psi_0}{\partial t}=d\Delta\psi_0+\vec{\nu}\nabla^3\psi_0-\delta\Delta^2\psi_0+\gamma(\nabla\psi_0)^2. \tag{12}$$

The important parameter is d:

$$d = D_{00} - \sum_{i>0} \frac{\vec{V}_{0i}\vec{V}_{i0}}{\lambda_i}. \tag{13}$$

The other parameters are

$$\vec{\nu} = \sum_{i>0} \frac{1}{\lambda_i}\left((D_{0i}\vec{V}_{i0} + \vec{V}_{0i}D_{i0}) - \vec{V}_{0i}\sum_{j>0} \frac{(\vec{V}_{ij}\vec{V}_{j0})}{\lambda_j}\right), \tag{14}$$

$$\delta = \sum_{i>0} \frac{1}{\lambda_i}\left(D_{0i}D_{i0} - \sum_{j>0} \frac{D_{0i}\vec{V}_{ij}\vec{V}_{j0} + D_{ij}\vec{V}_{j0}\vec{V}_{0i} + D_{j0}\vec{V}_{ij}\vec{V}_{0i}}{\lambda_j} + \sum_{j>0,k>0} \frac{(\vec{V}_{0i}\vec{V}_{ij})(\vec{V}_{jk}\vec{V}_{k0})}{\lambda_j\lambda_k}\right). \tag{15}$$

Note that d, $\vec{\nu}$, and δ depend only on the y and z components of the vector $\vec{\mathbf{V}}$. The coefficient in front of the nonlinear term γ can be found using the same argument as in Refs. [8, 11]. It is equal to $\gamma = -(c - V_{00,x})/2$.

A few observations are now in order. First, if all the components of the matrix $\vec{\mathbf{V}}$ are the same (the case of bulk flow), all terms $\vec{V}_{i0}$ and $\vec{V}_{0i}$ vanish for $i>0$, and after the coordinate change $x \mapsto x - V_{00,x}t$ Eq. (12) turns into the classic Kuramoto-Sivashinsky equation. Nontrivial effects of the external field thus appear only if the field induces a differential flow of the system species. Second, we have so far made no assumptions about the strength of the field: Eq. (12) and expressions (13), (14), and (15) are valid for arbitrary fields. Third, the parameters of Eq. (12), except for γ, depend explicitly only on the lateral component $\vec{\mathbf{V}}_{\|}$ of the flow/field. However, they depend on the normal component implicitly, through the eigenvectors $\mathbf{w}_i$ of the problem (4).

The most important observation is that the effective diffusion coefficient d, which determines the stability of the trivial solution $\psi_0 = 0$, depends quadratically on the strength of the lateral component of the field. If the sign of the additional term in Eq. (13) is opposite to that of D_{00}, a sufficiently strong lateral field *will always change the stability* of the front.

We now seek the explicit dependence of d on the normal component $\mathbf{V}_x$ of the flow field for small $\mathbf{V}_x$. Taking the operator $-\mathbf{V}_x(\partial/\partial\xi)$ as a perturbation and using perturbation theory one obtains

$$\mathbf{w}_0 = \mathbf{w}_0^0 - \sum_{i>0} \frac{\langle \mathbf{w}_i^0 | \mathbf{V}_x | \mathbf{w}_0^{0\prime}\rangle}{\lambda_0 - \lambda_i}\mathbf{w}_i^0 \equiv \mathbf{w}_0^0 + \sum_{i>0} \frac{\langle \mathbf{w}_i^0 | \mathbf{V}_x | \mathbf{w}_0^{0\prime}\rangle}{\lambda_i}\mathbf{w}_i^0, \tag{16}$$

where the zero superscripts designate the values corresponding to $\mathbf{V}_x = 0$. The expression (13) now becomes

$$d = D_{00}^0 + \sum_{i>0} \frac{\langle \mathbf{w}_i^0 | \mathbf{V}_x | \mathbf{w}_0^{0\prime}\rangle}{\lambda_i}(D_{i0}^0 + D_{0i}^0) - \sum_{i>0} \frac{\vec{V}_{0i,\|}\vec{V}_{i0,\|}}{\lambda_i}. \tag{17}$$

Equation (17) shows that the diffusion coefficient d depends linearly on the normal component of the field (as long as this component is small enough). Hence the field in one of the normal directions always has a stabilizing effect, while a field in the opposite direction destabilizes the front. In other words, when the original system is slightly subcritical (D_{00}^0 is small and positive, and the front is stable) applying the field in one normal direction will turn d negative and thus destabilize the front propagation. Conversely, in the slightly supercritical case ($D_{00}^0 < 0$), applying a field in the opposite direction will make $d>0$ and stabilize the front. This conclusion is valid for any system in a near-critical regime.

The following section illustrates these findings by numerical simulation of a system with cubic autocatalysis.

III. FRONT SIMULATIONS IN A SYSTEM WITH CUBIC AUTOCATALYSIS

While the considerations in the preceding section apply to both two and three spatial dimensions, we restrict ourselves here to a two-dimensional system. We model situations with either $V_x \neq 0$, $V_y = 0$, or $V_x = 0$, $V_y \neq 0$.

We study here a model autocatalytic chemical system $A + 2B \rightarrow 3B$. This model has often been used for studies of instabilities of reaction-diffusion fronts [11–13]. With advection of species A the system is described by the following equation:

$$\frac{\partial a}{\partial t} = -ab^2 + D_A\Delta a - \vec{V}\nabla a, \tag{18}$$

$$\frac{\partial b}{\partial t} = ab^2 + D_B\Delta b. \tag{19}$$

The system is described in a coordinate frame in which the species B does not undergo bulk motion.

Locally, the system has an integral $a + b = a_0$, which is an external parameter. The system has two steady states, ($a = a_0$, $b = 0$) and ($a = 0$, $b = a_0$), the former unstable and the latter stable. When spatially extended in one dimension ($D_A, D_B \neq 0$ $\vec{V} = 0$), the system supports steadily propagating waves of transition from the unstable state to the stable one [12] (Fig. 1). In a two- or three-dimensional medium, the propagating planar front remains stable as long as $D_A/D_B < \delta_{\rm cr} \approx 2.35$ [11,12].

We simulated the system (18), (19) in a 2D rectangular domain with lateral (i.e., in the direction of the planar front) size between 400 and 4800 units and normal length 100–200 units. The typical size of the medium was 1200×100 units. In these simulations the planar front extended in the horizontal (x) direction and propagated along the vertical (y) direction. We imposed periodic boundary conditions on the vertical edges of the domain and no flux boundary conditions on the horizontal edges.

A. Effects of lateral flow

All the simulations of the system with a differential flow of species along the front were made with equal diffusion coefficients. The calculations demonstrate that, in accordance with Eq. (17), the otherwise stable flat propagating

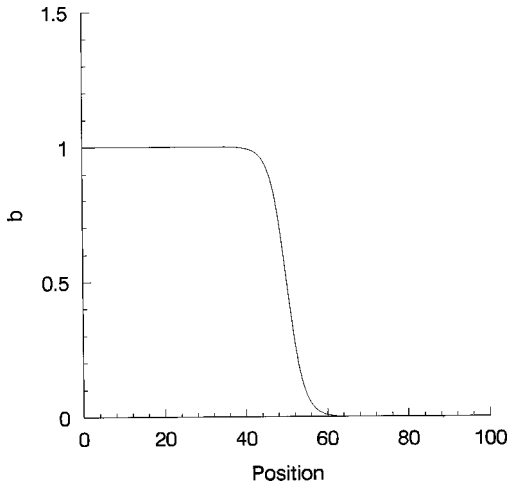

FIG. 1. Transition front between the initial ($a=1$, $b=0$) and final ($a=0$, $b=1$) states for the reaction $A+2B\rightarrow 3B$. All time and space units in this and subsequent figures are dimensionless.

front becomes unstable when a lateral field is imposed, provided that the field strength exceeds a critical value. Our numerical simulations also reveal details of the pattern development that are missing in the analysis performed in Sec. II. Figure 2(a) shows that the front becomes periodically modulated, and the modulation pattern drifts in the direction opposite to the flow of A induced by the field. The amplitude of the pattern grows roughly linearly with the differential flow velocity, as illustrated in Fig. 3. The jagged appearance of the curve results from the fact that the number of periods in the pattern, and hence the front characteristics, change in a discrete fashion as the parameters change continuously.

For larger flows, $2<v<10$, the amplitude of the front perturbation grew so large that the distortions caused the simulations to abort because the program could no longer locate and follow the front. At still larger flow velocities, the tendency is reversed: the amplitude of the front distortions diminishes as the velocity grows. The shape of the front

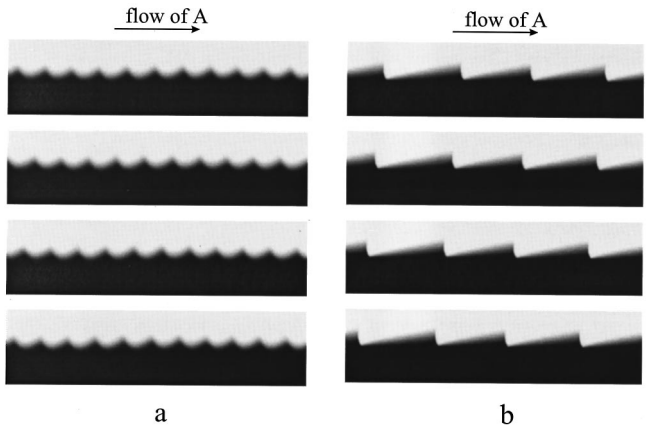

FIG. 2. Cellular patterns caused by lateral differential flow of reacting species. The size of the system is 1200×100 units. Gray levels represent concentration of A: dark areas correspond to high a. The front propagates downwards. Time increases from the top down. Parameters: $D_A=D_B=2.0$. (a) Flow velocity $V_x=0.7$; successive frames are 100 time units apart. (b) Flow velocity $V_x=50$; successive frames are 20 time units apart.

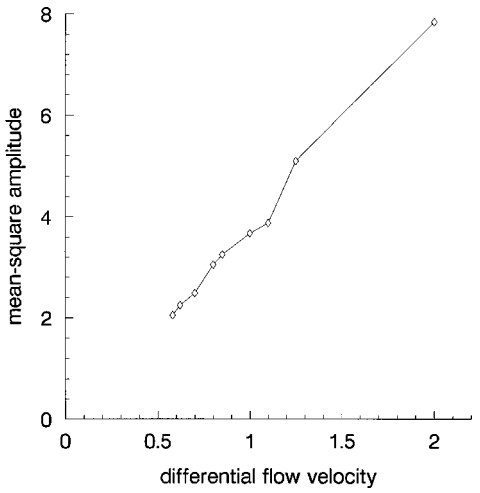

FIG. 3. Mean-square amplitude of the cellular pattern as a function of the lateral differential flow velocity. Parameters: $D_A=D_B=2.0$.

modulation becomes highly asymmetric [Fig. 2(b)].

As shown in Fig. 4, the lateral differential flow significantly affects the velocity of the front propagation. During the transient period, the growth of the front propagation velocity accompanied the perturbation growth and was barely noticeable at the early stages. The lateral field affects the lateral drift of the front patterns as well: the drift also increases with the differential flow velocity (Fig. 4).

B. Effects of normal flow

While the effects of a lateral flow appeared in the model with equal diffusion coefficients, and hence far from the diffusive front instability, the destabilizing effects of a normal flow were only observed in a vicinity of the diffusive instability, with $D_A/D_B=\delta_{cr}\approx 2.35$.

Figure 5 shows a cellular pattern that emerges on an otherwise stable planar front ($D_A/D_B<\delta_{cr}$) due to the normal differential flow of species. Just as in the case of lateral flow, the pattern amplitude grows with the strength of the external

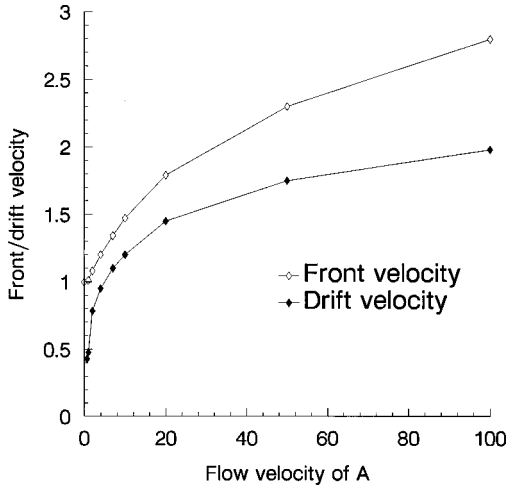

FIG. 4. Front propagation velocity and drift velocity of the cellular pattern versus lateral differential flow velocity. Parameters: $D_A=D_B=2.0$.

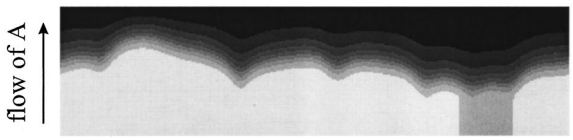

FIG. 5. Cellular pattern appearing on an initially flat front as the result of normal differential flow. Parameters: $D_A=5$, $D_B=2.2$, $v=0.225$. The front propagates upward.

field (Fig. 6). Unlike the case of lateral flow, the pattern does not drift along the front. An increase of the normal flow of A in the positive direction (up in Fig. 5) slows the front until the front undergoes a transition to another state. This new state represents a nearly linear decrease of b and increase of a along the y direction. The critical flow velocity in our case was $V_{cr}\approx 0.25$.

Figure 7 illustrates the opposite situation. Under slightly different conditions, $D_A/D_B=2.94>\delta_{cr}$, the planar front forms cellular patterns through a diffusive instability. Imposing an external field in the direction opposite to that in the previous example makes the cellular pattern disappear and the front become flat. The flow of A in the negative direction accelerates the front propagation (Fig. 8). It should be noted that the dependence of the front velocity on the normal flow velocity remained qualitatively the same, and the phenomenon of front extinction mentioned above persisted, even when the diffusion coefficient ratio was far from critical (e.g., for $D_A=D_B=2$).

IV. NUMERICAL PROCEDURES

Two considerations influenced our choice of a numerical integration method. One is that the necessity of shifting the frame to adjust to the front position rules out multistep techniques, such as the Gear or Adams and related predictor-corrector methods, because a frame shift represents a kind of a singular perturbation to the numerical procedure. The other is that neither the kinetic nor the diffusive terms in the equations make the problem stiff: the kinetic terms in the equation for a and b are exactly equal in absolute value, and the

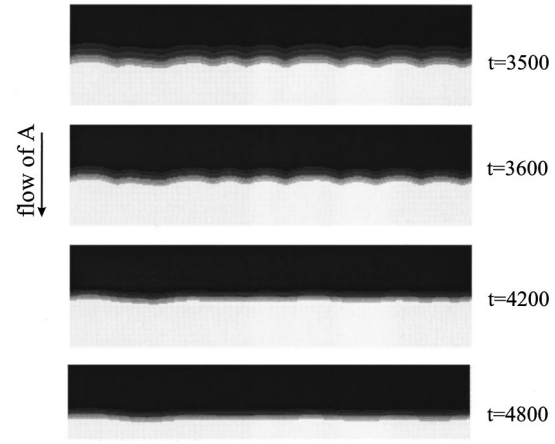

FIG. 7. Flattening of a cellular front by a normal differential flow. The upper panel shows the front immediately before the switching on of the flow. Parameters: $D_A=5.0$, $D_B=1.7$. The front propagates upward.

diffusive terms in the discretized scheme must be kept small because of the steep gradients in the solutions. The possibility of numerical instability caused by the convective term can be avoided by using an ''upwind'' scheme in order to discretize the first order spatial derivative: forward differences for positive flow velocities and backward differences for negative velocities [14]. These observations, combined with the relatively modest demands for numerical accuracy, led us to choose the Euler technique as an adequate tool for the problem. We varied both the time and the space resolutions to test the validity of the results. The size of the two-dimensional spatial grid was changed from 400 to 800 mesh points in the x dimension and from 100 to 200 in the y dimension. The time step was varied from 10^{-3} to 10^{-2}. The frame adjustment to the front was made so that the level of the a variable ($a\leqslant 0.5$) was kept at a fixed distance from the boundary $a=1$ (normally half of the system size in the y dimension). At the start of each run, the propagating front was precalculated in a 1D system and then extended in the second (x) dimension with a random shift along the y dimension. The amplitude of the shift was 3 units, i.e., no more

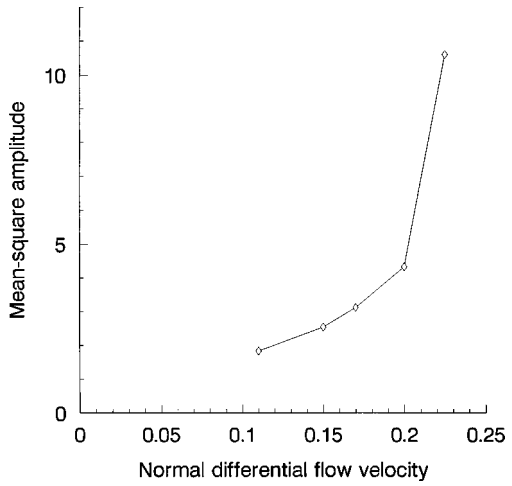

FIG. 6. Mean-square amplitude of the cellular pattern as a function of normal differential flow velocity. Parameters: $D_A=5$, $D_B=2.2$. The front propagates in the positive direction.

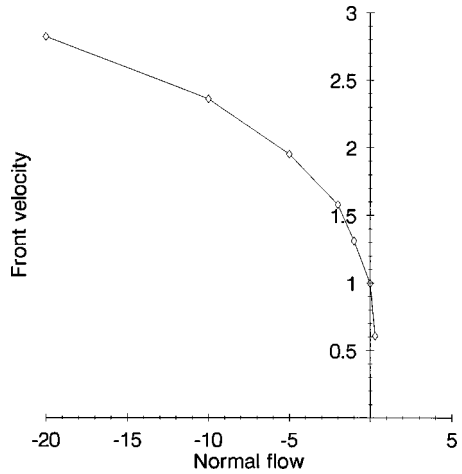

FIG. 8. Front propagation velocity versus normal differential flow velocity. Parameters: $D_A=5$, $D_B=2.2$. The front propagates in the positive direction.

than 3% of the system size. To calculate the mean-square amplitude of the front pattern, the front line was taken as the set of coordinates where $a=0.5$.

V. DISCUSSION

An interesting feature of the periodic patterns emerging on the front is that they always drift against the flow of the A component. In terms of an ''activator-inhibitor'' description, the A species may be considered an inhibitor. It was argued recently [15] that it is typical for waves induced by a differential flow instability in activator-inhibitor systems to move against the flow of inhibitor. Apparently, the front cellular patterns induced by a differential flow preserve this feature.

The front propagation phenomena shown by model (18), (19) are sometimes considered as analogs of flame fronts [3,12]. We note one peculiarity of the cubic autocatalysis in model (18), (19): its initial state $a=a_0$ and $b=0$, which corresponds to the extinguished state, is unstable. Therefore one cannot observe extinction of a front in the simulations. As mentioned in Sec. III B, we observed a transition from a relatively narrow front to a nearly linear gradient when a normal field was applied. We believe that in a more realistic model, with the extinguished state stable against subthreshold perturbation, such a transition would correspond to extinguishing the front.

Chemical waves in electric fields have been studied previously [6], but the explanations of the observed phenomena were restricted to a one-dimensional description of the wave-field interaction [16]. As shown here, the effects of external fields on fronts in two- or three-dimensional systems may be much richer.

It is well known that the physical nature of the Turing instability is determined by the fact that the fast diffusion of the inhibitor removes it from the spot of increased activator growth [17]. The nature of the front instability due to normal flow appears to be similar: the front becomes unstable when the inhibitor, species A in our model, is taken away from the reaction zone by the flow, and the front's stability increases in the opposite case. It should be noted that the term ''inhibitor'' has a rather narrow meaning in the context of Turing instabilities: a small deviation of the inhibitor concentration from its steady state value counteracts a small deviation of the activator concentration of the same sign from the activator's steady state. In general, this does not prevent the inhibitor species from accelerating the steady state reaction rate. In fact, this is the case in model (18), (19): the rate of the reaction increases with the concentration of species A. The acceleration of the front with the flow of A pointing towards the front can now be understood: it is caused by the increased steady state rate of the reaction $A\rightarrow B$. While the effect of a normal field on the front propagation velocity does not seem counterintuitive, the similarly strong effect of a lateral field appears somewhat surprising. The above explanation of the front acceleration under normal flow can also be applied in this case to rationalize the phenomenon of the pattern drift. When perturbations of the front develop, some parts of the distorted front are facing the flow: the flow has a normal component with respect to these parts, and the parts start drifting in the direction opposite to the flow. This consideration, however, does not elucidate the mechanism of the instability itself, nor does it explain the acceleration of the front due to lateral flow. We believe that a more thorough study of Eq. (12) should provide some clue as well as describe the emerging front patterns. Since Eq. (12) is quite complicated, such a study will be a demanding task.

Our results suggest the possibility of controlling propagating fronts by external fields. In particular, the potential to accelerate and/or stabilize front propagation may be important for combustion applications. We find it interesting that the effects described here seem to be similar in many respects to those found by Sher *et al.* [7] in a study of flames in electric fields. The possibility of stabilizing fronts may also be significant for electrophysiology, and particularly for studies of excitation waves in cardiac muscle.

To simulate an infinite medium with a finite grid we employed the standard approach of using periodic boundary conditions: we performed our simulations with periodic boundary conditions in the lateral dimension. More realistic boundary conditions would certainly affect the results. In particular, the convective nature of the front instability due to lateral fields will become important, and it merits further study.

ACKNOWLEDGMENTS

We gratefully acknowledge the support of the National Science Foundation Chemistry Division and the W. M. Keck Foundation.

[1] A. Baylyss and B. J. Matkowsky, Prog. Astronaut. Aeronaut. **173**, 157 (1997).

[2] *Handbook of Crystal Growth*, edited by D. T. J. Hurle (Elsevier, Amsterdam, 1993); J. S. Langer, Rev. Mod. Phys. **52**, 1 (1980).

[3] *Chemical Waves and Patterns*, edited by R. Kapral and K. Showalter (Kluwer Academic, Dordrecht, 1995).

[4] A. B. Rovinsky and M. Menzinger, Phys. Rev. Lett. **69**, 1193 (1992); **70**, 778 (1993); **72**, 2017 (1994).

[5] V. Krinsky, E. Hamm, and V. Voignier, Phys. Rev. Lett. **76**, 3854 (1996); A. Pumir and V. I. Krinsky, Physica D **91**, 205 (1996).

[6] H. Sevcikova, I. Schreiber, and M. Marek, J. Phys. Chem. **100**, 19 153 (1996); H. Sevcikova, M. Marek, and S. C. Mueller, Science **257**, 951 (1992); O. Steinbock, J. Schultze, and S. C. Mueller, Phys. Rev. Lett. **68**, 248 (1992); H. Sevcikova and M. Marek, Physica D **9**, 140 (1983); R. Feeney, S. L. Schmidt, and P. Ortoleva, *ibid.* **2**, 536 (1981).

[7] E. Sher, G. Pinhasi, A. Pokryvailo, and R. Bar-On, Combust. Flame **94**, 244 (1993).

[8] Y. Kuramoto and T. Tsuzuki, Prog. Theor. Phys. **55**, 356 (1976); G. I. Sivashinsky, Combust. Sci. Technol. **15**, 137 (1977).

[9] Y. Kuramoto, *Chemical Oscillations, Waves, and Turbulence*

(Springer-Verlag, New York, 1984).
[10] S. K. Scott and K. Showalter, J. Phys. Chem. **96**, 8702 (1992).
[11] A. Malevanets, A. Careta, and R. Kapral, Phys. Rev. E **52**, 4724 (1995).
[12] D. Horvath, V. Petrov, S. K. Scott, and K. Showalter, J. Phys. Chem. **98**, 6332 (1993).
[13] Z. Zhang and S. A. Falle, Proc. R. Soc. London, Ser. A **446**, 1 (1994).
[14] W. H. Press, S. A. Teukolsky, W. T. Vetterling, and B. P. Flannery, *Numerical Recipes in C*, 2nd ed. (Cambridge University Press, Cambridge, England, 1992).
[15] A. B. Rovinsky, S. Nakata, V. Z. Yakhnin, and M. Menzinger, Phys. Lett. A **216**, 262 (1996).
[16] S. L. Schmidt and P. Ortoleva, J. Chem. Phys. **67**, 3771 (1977).
[17] L. Segel and J. L. Jackson, J. Theor. Biol. **37**, 545 (1972); H. Meinhardt, *Models of Biological Pattern Formation* (Academic Press, New York, 1982).